Chinese Chemical Letters 31 (2020) 2041–2044

Contents lists available at ScienceDirect

Chinese Chemical Letters

journal homepage: www.elsevier.com/locate/cclet

Communication

Highly sensitive acetone gas sensor based on ultra-low content bimetallic PtCu modified $WO_3 \cdot H_2O$ hollow sphere

Lifeng Deng, Liping Bao, Jingcheng Xu, Ding Wang*, Xianying Wang

College of Materials Science and Engineering, University of Shanghai for Science & Technology, Shanghai 200093, China

ARTICLE INFO

Article history:
Received 6 February 2020
Received in revised form 30 March 2020
Accepted 19 April 2020
Available online 22 April 2020

Keywords:
Bimetallic nanocrystal
$WO_3 \cdot H_2O$ hollow spheres
Two-dimensional materials
Acetone gas sensors
Nanocomposites

ABSTRACT

Acetone is an important industrial raw material as well as biomarker in medical diagnosis. The detection of acetone has great significance for safety and health. However, high selectivity and low concentration (ppb level) detection remain challenges for semiconductor gas sensor. Herein, we present a novel sensitive material with bimetallic PtCu nanocrystal modified on $WO_3 \cdot H_2O$ hollow spheres (HS), which shows high sensitivity, excellent selectivity, fast response/recovery speed and low limit of detection (LOD) to acetone detection. Noteworthy, the response (R_a/R_g) of $WO_3 \cdot H_2O$ HS sensor increased by 9.5 times after modification with 0.02% bimetallic PtCu nanocrystals. The response of PtCu/$WO_3 \cdot H_2O$ HS to 50 ppm acetone is as high as 204.9 with short response/recovery times (3.4 s/7.5 s). Finally, the gas-sensitivity mechanism was discussed based on gas sensitivity test results. This research will offer a new route for high efficient acetone detection.

Acetone is an important industrial raw material as well as an important biomarker in medical diagnosis [1]. Therefore, the detection of acetone has great significance for safety and health. The clinical data showed that the acetone was an important breath biomarker for noninvasive diagnosis of human type-1 diabetes and the concentration for exhaled diabetes exceeded 1.8 ppm, while that for healthy people was 0.3–0.9 ppm [2]. Therefore, high selectivity and low concentration (ppb level) acetone detection will be requested for application. The pure $WO_3 \cdot H_2O$ rarely reported for acetone gas detection due to low acetone sensitivity and poor selectivity. There are several methods to improve sensing performances such as the design of micro-structures [3], the regulation of defects [4], the generation of p-n junction [5], and the modification of precious metals [6]. Among them, noble metal modification including electronic or/and chemical sensitization, has become a very important modification strategy [7]. However, the usage of noble metal increases sensor's cost. Therefore, the use of common metals instead of noble metals and the reduction of loading amount are beneficial for the application of gas sensor. Compared with single metal modification, bimetal modification has both electronic and chemical sensitization effects by selecting the optical metals [8]. Pt nanoparticles (NPs) are usually used as a chemical sensitizing material because of its excellent catalytic properties and O_2 spillover effects [9]. As a cheap material, Cu or Cu_xO also shows unique catalytic properties and electronic sensitization effect [10]. Therefore, it is possible to achieve both sensitization by preparing PtCu bimetallic nanocrystals, which can improve their gas sensitivity and selectivity simultaneously. In addition, ultra-low content PtCu modification hardly add to sensor prices.

In this work, the PtCu NPs and $WO_3 \cdot H_2O$ hollow sphere (HS) were prepared first. And then, the PtCu/$WO_3 \cdot H_2O$ HS was prepared by impregnation method. Their structure, morphology and surface chemical state were characterized by X-ray power diffraction (XRD), scanning electron microscopy (SEM), transmission electron microscopy (TEM) and X-ray photoelectron spectroscopy (XPS), and their sensing properties were measured. In addition, the optical loading amount of PtCu on nanocomposites was further studied. Based on gas sensitivity test results, the sensing mechanism was discussed and the utilization potentiality was illuminated by comparing with recent works.

The preparation schematic illustration of PtCu/$WO_3 \cdot H_2O$ HS is displayed in Fig. S1 (Supporting information). The $WO_3 \cdot H_2O$ HS was first obtained by a simple hydrothermal method. And then, the bimetallic PtCu NPs were synthesized by liquid phase chemical method [11]. Finally, different amount of PtCu NPs were modified on $WO_3 \cdot H_2O$ HS by impregnation method.

The crystalline structure of $WO_3 \cdot H_2O$ HS and 0.02% PtCu/$WO_3 \cdot H_2O$ HS was characterized by XRD. As shown in Fig. 1, the diffraction pattern of both the original $WO_3 \cdot H_2O$ HS and 0.02%

* Corresponding author.
E-mail address: wangding@usst.edu.cn (D. Wang).

https://doi.org/10.1016/j.cclet.2020.04.033

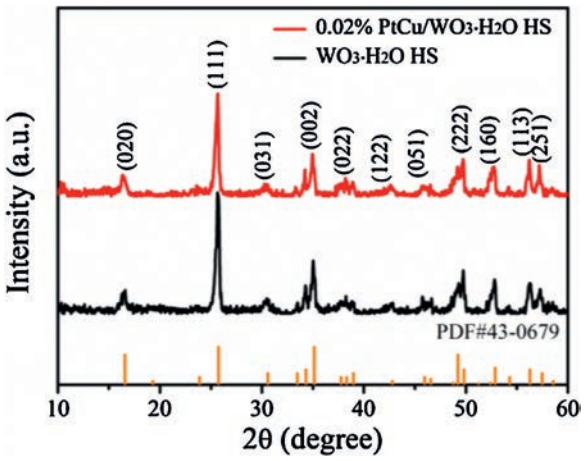

Fig. 1. XRD patterns of $WO_3·H_2O$ HS and 0.02% PtCu/$WO_3·H_2O$ HS.

PtCu/$WO_3·H_2O$ HS could be indexed to orthorhombic $WO_3·H_2O$ (JCPDS card No. 43-0679), and no other impurities peaks could be found, proving it to be of high purity [12]. We cannot observe diffraction peaks of Cu or Pt for the 0.02% PtCu/$WO_3·H_2O$ HS due to ultralow content of PtCu NPs in the nanocomposite.

SEM and TEM characterizations were used for studying the morphology of sensitive materials. Obviously, the uniform sphere self-assembled by nanosheets are observed in the Fig. 2a. In Fig. 2b, the spherical $WO_3·H_2O$ has a bright and dark contrast between central and edges, which further proves the hollow spherical structure, and the result is well consistent with SEM image. HR-TEM image of $WO_3·H_2O$ HS was displayed in the inset of Fig. 2b. The interplanar distances are 0.26 nm and 0.35 nm, which correspond to the (200) and (111) crystal planes of orthorhombic $WO_3·H_2O$, respectively [13]. The TEM and HR-TEM images of PtCu nanoparticles are shown in Fig. 2c. Nanoparticles with evenly distribution can be observed in the TEM image. In addition, the (200) plane of Cu and (111) crystal plane of Pt can be noticed in the high resolution transmission electron microscopy (HR-TEM) image [14]. The characterization results show that bimetallic PtCu nanocrystals were prepared successfully. As shown in Figs. 2d and e, the hollow spherical structure still maintain after modification with bimetallic PtCu nanocrystals. The co-existence of (200) plane of Cu, (111) crystal plane of Pt and (111) plane of $WO_3·H_2O$ in the Fig. 2f indicate that PtCu/$WO_3·H_2O$ HS was prepared successfully [15].

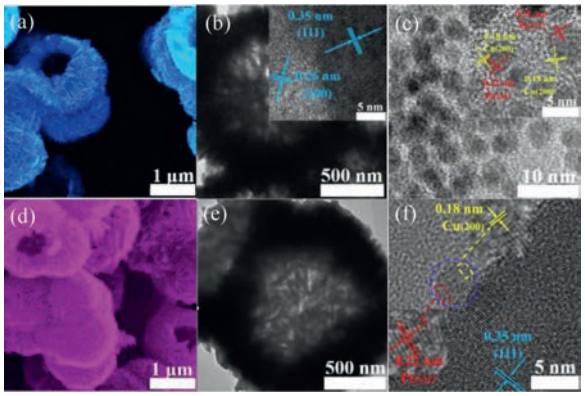

Fig. 2. (a) SEM and (b) TEM images of $WO_3·H_2O$ HS. (c) TEM and HR-TEM images of PtCu NPs. (d) SEM and (e) TEM images of 0.02% PtCu/$WO_3·H_2O$ HS. (f) HR-TEM image of 0.02% PtCu/$WO_3·H_2O$ HS.

The operating temperature has an important effect on the adsorption oxygens on the surface of sensitive materials, and thus affects their sensitivity [16]. In addition, the loading amounts of PtCu also has a great influence on the gas sensitivity. The low PtCu content leads to insufficient active sites on the gas sensitive material. However, the excessive amount of catalysts enlarge the depletion layer, which was formed around the catalyst, can be overlapped, leading to the deterioration of catalytic effect [17,18]. Responses of sensors based on pure $WO_3·H_2O$ HS and PtCu/$WO_3·H_2O$ HS with different PtCu loading amounts toward 50 ppm acetone at different operating temperatures were displayed in Fig. 3a. Clearly, all sensors based on PtCu/ $WO_3·H_2O$ HS with different PtCu loading amounts show higher response value than $WO_3·H_2O$ HS. In addition, the response value of $WO_3·H_2O$ HS sensor increased from 21.6–88.3 for 0.01% PtCu/$WO_3·H_2O$ HS, 180.9 for 0.015% PtCu/$WO_3·H_2O$ HS, 204.9 for 0.02% PtCu/$WO_3·H_2O$ HS, 116.1 for 0.025% PtCu/$WO_3·H_2O$ HS, and 81.8 for 0.03% PtCu/$WO_3·H_2O$ HS, respectively. The maximum response value of 0.02% PtCu/$WO_3·H_2O$ HS sensor (204.9) is 9.5 times than that of original $WO_3·H_2O$ HS sensor (21.6). Fig. 3b shows that all sensors have fast response/recovery speed. The response/recovery times of 0.02% PtCu/$WO_3·H_2O$ HS and the original $WO_3·H_2O$ HS sensor are 3.4/7.5 s and 3.6/5.7 s. The slight increase of recovery time is due to the decrease in operating temperature from 300 °C to 280 °C. Besides, the response values of 0.02% PtCu/$WO_3·H_2O$ HS sensor remained almost same after 7 cycles of testing (Fig. 3c), which proves good stability and repeatability of the sensor. Selectivity is also an important indicator for measuring the anti-interference ability of sensors, and we tested responses of eight different volatile organic chemicals (VOCs) to evaluate the selectivity of sensors. As shown in Fig. 3d, the response value of 0.02% PtCu/$WO_3·H_2O$ HS sensor to acetone is much higher than other gases, which proves that our sensor has excellent acetone selectivity. The dynamic response of the gas sensors based on $WO_3·H_2O$ HS and 0.02% PtCu/$WO_3·H_2O$ HS at 280 °C was shown in Fig. 3e. The dynamic responses show a gradual increase with increasing acetone concentration from 0.01 ppm to 100 ppm. The response of $WO_3·H_2O$ HS sensor to different concentration of acetone was compared with 0.02% PtCu/$WO_3·H_2O$ HS sensor. As shown in Fig. S2 (Supporting information), the response of $WO_3·H_2O$ HS sensor was improved obviously by modification 0.02% PtCu nanocrystal. In addition, the limit of detection was improved from 0.5 ppm to 0.01 ppm, which is a significant performance improvement. As the breath biomarker of human type-1 diabetes, the ppb level detection to acetone is essential for noninvasive diagnosis. Therefore, the dynamic response and the relationship curves of 0.02% PtCu/$WO_3·H_2O$ HS to low acetone concentration (10–1000 ppb) was further studied. A clear stepwise increasing trend from 10 ppb to 500 ppb was shown in the inset of Fig. 3e. For better application, the relationship between the reaction value and the acetone concentration was studied. As shown in Fig. 3f, the relationship between the S-1 and acetone concentrations (C_g) was fitted in the double logarithm coordinate, which showed a good linear relationship (0.01–100 ppm) [19]. Furthermore, we can speculate the adsorption oxygen species on the surface of the material through this linear relationship fitting equations:

$$S = 1 + \alpha C_g^{\beta} \quad (1)$$

$$\lg(S\text{-}1) = \lg\alpha + \beta \lg C_g \quad (2)$$

where α is the prefactor and β is the surface species charge parameter. According to reports [20], when β is 0.5, the type of adsorbed oxygen ions on the surface of the material is O^{2-}, but when β is 1, the type of adsorbed oxygen ions change to O^- [20].

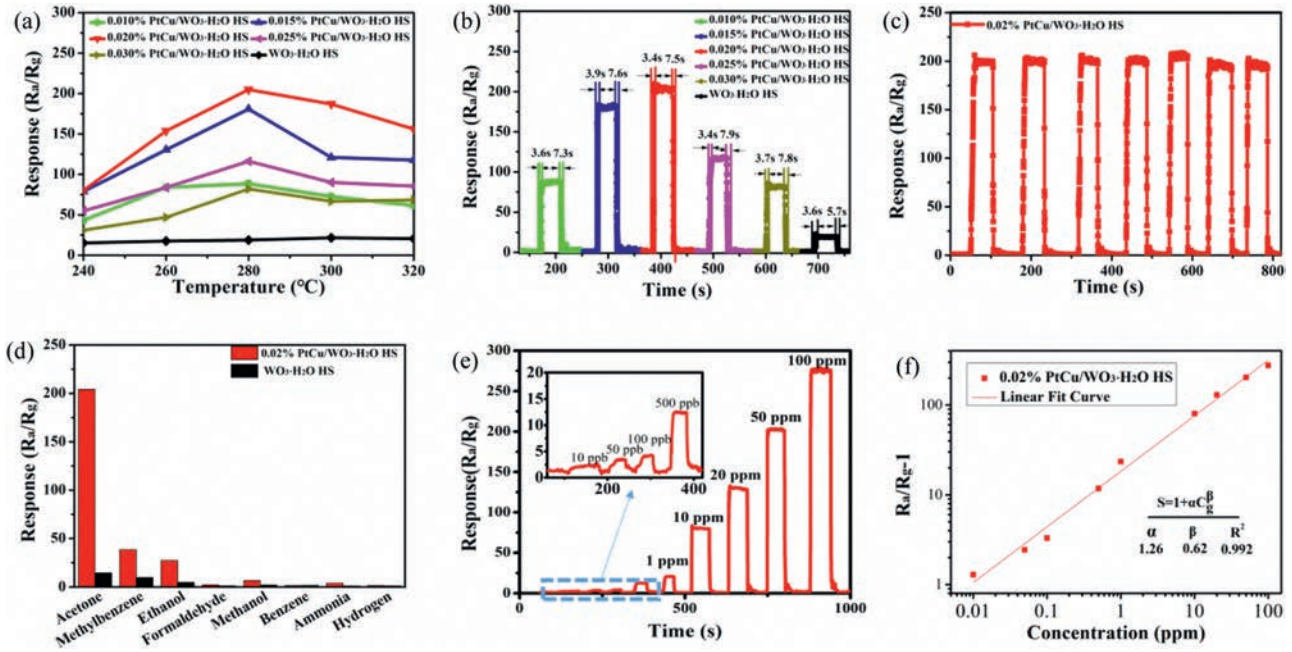

Fig. 3. (a) Responses of sensors based on pure $WO_3{\cdot}H_2O$ HS and PtCu/$WO_3{\cdot}$ H_2O HS with different PtCu loading amounts toward 50 ppm acetone at different operating temperatures. (b) Response/recovery curves of sensors based on pure $WO_3{\cdot}H_2O$ HS and PtCu/$WO_3{\cdot}H_2O$ HS with different PtCu loading amounts toward 50 ppm acetone at 280 °C. (c) The reproducibility of sensor based on 0.02% PtCu/$WO_3{\cdot}H_2O$ HS to 50 ppm acetone. (d) The selectivity of sensors based on pure $WO_3{\cdot}$ H_2O HS and PtCu/$WO_3{\cdot}H_2O$ HS to 50 ppm different reference gases at 280 °C. (e) The dynamic response and (f) the relationship curves of the gas sensors based on 0.02% PtCu/$WO_3{\cdot}H_2O$ HS at 280 °C.

The β values of 0.020% PtCu/$WO_3{\cdot}H_2O$ HS is 0.62. Therefore, the main type of adsorbed oxygen ions may be O^{2-}. The good linear relationship between response and acetone concentration illustrated that 0.02% PtCu/$WO_3{\cdot}H_2O$ HS sensor could be used in both ppm and ppb levels acetone detection.

Generally, the sensing performance of metal oxide semiconductor (MOS) mainly depends on the chemical reaction between gas molecules and their surface adsorbed oxygen, which causes the change of charge depletion layer and further results in the change of resistance value [21]. The adsorbed oxygen (O_2^-, O^- and O^{2-}) is generated by chemical adsorption of oxygen on the surface of MOS, and the main types of oxygen ions on the surface of the material are related to the operating temperature [22]. In this work, the optimal operating temperature of 0.02% PtCu/$WO_3{\cdot}H_2O$ HS sensor is 280 °C. Combined with the calculation result of β value, we can infer that the form of oxygen ions on the materials surface may be O^{2-} and a small amount of O^- [19]. The W 4f and O 1s XPS of $WO_3{\cdot}H_2O$ HS and 0.02% PtCu/$WO_3{\cdot}H_2O$ HS are shown in Fig. S3 (Supporting information). Both the $WO_3{\cdot}H_2O$ HS and 0.02% PtCu/$WO_3{\cdot}H_2O$ HS have the similar W 4f XPS spectra. The peaks with binding energy at 530.6 eV and 532.7 eV are correspond to lattice oxygen (O_{lat}) and adsorbed oxygen (O_{ads}) [23], respectively. By calculation, the percentage of adsorbed oxygen in the original $WO_3{\cdot}H_2O$ HS was 27.6%, but this proportion rose to 31.9% after modification with PtCu NPs. The enhanced adsorbed oxygen percentage may be due to the spillover effect of O_2 on PtCu NPs. In addition, Pt and Cu can react with O_2 in the air to form p-type metal oxides [24,25]. The p-n junction will form between PtCu NPs and n-type $WO_3{\cdot}H_2O$ HS, which will hinder electron transport and further increase the resistance of the material [26–28]. Fig. 4 shows reaction mechanism of 0.02% PtCu/$WO_3{\cdot}H_2O$ HS after acetone gas are injected into the air chamber. Acetone molecules will react with O^- or O^{2-}, and the released electrons will back to the sensitive material. The reaction equation can be described as follows [29]:

$$CH_3COCH_{3(gas)} + 8O^-/8O^{2-}{}_{(ads)} \rightarrow 3CO_2 + 3H_2O + 8e^-/16e^- \quad (3)$$

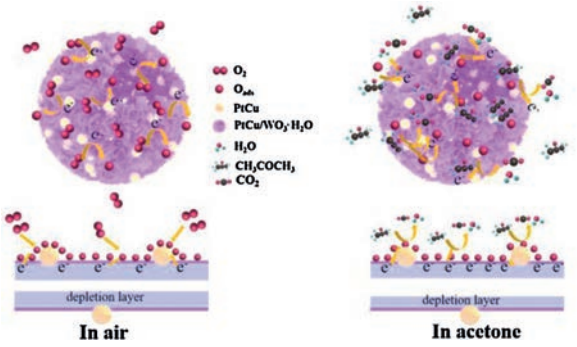

Fig. 4. Reaction mechanism schematic of 0.02% PtCu/$WO_3{\cdot}H_2O$ HS to acetone gas.

which will reduce the electron depletion layer and reduce the resistance value. Besides, PtO_x and Cu_xO will be reduced to PtCu NPs, making the material resistance value is further decrease, and the synergy between Pt and Cu may be another important reason affecting the gas-sensing performance.

In conclusion, the PtCu NPs and $WO_3{\cdot}H_2O$ HS were first prepared by liquid phase chemistry and hydrothermal methods. Then, PtCu/$WO_3{\cdot}H_2O$ HS were prepared by impregnating method. The optimum loading amount of PtCu was as low as 0.02%. The gas sensitivity test results show that the 0.02% PtCu/$WO_3{\cdot}H_2O$ HS sensor has high sensitivity (204.9 tower 50 ppm CH_3COCH_3), good selectivity and fast response/recovery speeds (3.4 s/7.5 s), low detection limit (0.01 ppm) and good stability. The enhanced sensing performance was attributed to the synergy between PtCu and $WO_3{\cdot}H_2O$, including the unique spillover effect of PtCu, the regulated depletion layer by p-type PtO_x and Cu_xO to n-type $WO_3{\cdot}H_2O$, and their selective catalysis to acetone. This research provides an important basis for the acetone biomarker detection, and provides important reference for the study of ultra-low content modification of materials.

Declaration of competing interest

The authors declare that they have no known competing financial interests or personal relationships that could have appeared to influence the work reported in this paper.

Acknowledgments

We greatly appreciate the financial supports from the National Natural Science Foundation of China (Nos. 51702212, 51802195, 31701678, 61671284), Science and Technology Commission of Shanghai Municipality (Nos. 18511110600, 19ZR1435200), Innovation Program of Shanghai Municipal Education Commission (No. 2019-01-07-00-07-E00015), Program of Shanghai Academic Research Leader (No. 19XD1422900).

Appendix A. Supplementary data

Supplementary material related to this article can be found, in the online version, at doi:https://doi.org/10.1016/j.cclet.2020.04.033.

References

[1] G. Li, Z. Cheng, Q. Xiang, et al., Sens. Actuator. B –Chem. 283 (2019) 590–601.
[2] R. Zhang, J.W. Shi, T.T. Zhou, et al., J. Colloid Interface Sci. 539 (2019) 490–496.
[3] L.L. Wang, S. Chen, W. Li, et al., Adv. Mater. 31 (2019) 1804583.
[4] W.C. Wang, F.Q. Liu, B. Wang, et al., Chin. Chem. Lett. 30 (2019) 1261–1265.
[5] Q. Rong, Y. Zhang, K. Li, et al., Mater. Res. Bull. 115 (2019) 55–64.
[6] D.S. Xu, P.C. Xu, X.Q. Wang, et al., ACS Appl. Mater. Interfaces 12 (2020) 8091–8097.
[7] S.J. Choi, I. Lee, B.H. Jang, et al., Anal. Chem. 85 (2013) 1792–1796.
[8] J.S. Jang, S.J. Kim, S.J. Choi, et al., Nanoscale 7 (2015) 16417–16426.
[9] V.V. Kondalkar, L.T. Duy, H. Seo, et al., ACS Appl. Mater. Interfaces 11 (2019) 25891–25900.
[10] Y.L. Chen, Z.R. Shen, Q.Q. Jia, et al., RSC Adv. 6 (2016) 2504–2511.
[11] C. Wang, C. Lin, L. Zhang, et al., Chemistry 20 (2014) 1753–1759.
[12] S.L. Liu, W. Zeng, Y.Q. Li, Mater. Lett. 253 (2019) 42–45.
[13] F. Li, S. Guo, J. Shen, et al., Sens. Actuator. B –Chem. 238 (2017) 364–373.
[14] F. Yang, J. Ye, Q. Yuan, et al., Adv. Funct. Mater. (2020) 1908235.
[15] H.H. Li, Q.Q. Fu, L. Xu, et al., Energy Environ. Sci. 10 (2017) 1751–1756.
[16] X. Xin, Y. Zhang, X. Guan, et al., ACS Appl. Mater. Interfaces 11 (2019) 9438–9447.
[17] A. Kolmakov, D.O. Klenov, Y. Lilach, et al., Nano Lett. 5 (2005) 667–673.
[18] M.H. Kim, J.S. Jang, W.T. Koo, et al., ACS Appl. Mater. Interfaces 10 (2018) 20643–20651.
[19] D. Wang, L. Tian, H. Li, et al., ACS Appl. Mater. Interfaces 11 (2019) 12808–12818.
[20] D. Wang, S. Huang, H. Li, et al., Sens. Actuator. B –Chem. 282 (2019) 961–971.
[21] S. Zhao, Y. Shen, P. Zhou, et al., Sens. Actuator. B –Chem. 282 (2019) 917–926.
[22] K. Wan, D. Wang, F. Wang, et al., ACS Appl. Mater. Interfaces 11 (2019) 45214–45225.
[23] J.C. Dupin, D. Gonbeau, P. Vinatier, et al., Phys. Chem. Chem. Phys. 2 (2000) 1319–1324.
[24] J. Ma, Y. Ren, X. Zhou, et al., Adv. Funct. Mater. 28 (2018) 1705268.
[25] Y.M. Choi, S.Y. Cho, D. Jang, et al., Adv. Funct. Mater. 29 (2019) 1808319.
[26] H.C. Ji, W. Zeng, Y.Q. Li, Nanoscale 11 (2019) 22664–22684.
[27] X.R. Zhou, X.W. Cheng, Y.H. Zhu, et al., Chin. Chem. Lett. 29 (2018) 405–416.
[28] L.J. Zhao, K. Wang, W. Wei, et al., InfoMat 1 (2019) 407–416.
[29] W. Liu, Y. Xie, T. Chen, et al., Sens. Actuator. B –Chem. 298 (2019) 126871.